

1 **Comparative analysis reveals the modular functional build-up of megaplasmid pTTS12**  
2 **of *Pseudomonas putida* S12: a paradigm for transferable traits, plasmid stability and**  
3 **inheritance?**

4 Hadiastri Kusumawardhani<sup>†</sup>, Rohola Hosseini<sup>†</sup>, Johannes H. de Winde\*

5 Institute of Biology Leiden, Leiden University, The Netherlands

6 <sup>†</sup>H. K. and R. H. contributed equally to this work.

7 \*Correspondence: [j.h.de.winde@biology.leidenuniv.nl](mailto:j.h.de.winde@biology.leidenuniv.nl)

8

9 **Running title:** Comparative analysis and elucidation of pTTS12 function

10 **Keywords:**

11 *Pseudomonas putida*, genome sequence, solvent tolerance, megaplasmid, mobile genetic elements

12

13 **Abstract**

14 The *Pseudomonas putida* S12 genome contains 583 kbp megaplasmid pTTS12 that carries over 600  
15 genes enabling tolerance to various stress conditions, including the solvent extrusion pump SrpABC.

16 We performed a comparative analysis of pTTS12 against 28915 plasmids from NCBI databases. We  
17 investigated putative roles of genes encoded on pTTS12 and further elaborated on its role in the  
18 establishment and maintenance of several stress conditions, specifically focusing on solvent tolerance  
19 in *P. putida* strains. The backbone of pTTS12 was found to be closely related to that of the  
20 carbapenem-resistance plasmid pOZ176, member of the IncP-2 incompatibility group, although  
21 remarkably the carbapenem resistance cassette is absent from pTTS12. Megaplasmid pTTS12 contains  
22 multiple transposon-flanked cassettes mediating resistance to various heavy metals such as tellurite,  
23 chromate (Tn7), and mercury (Tn5053 and Tn5563). Additionally, pTTS12 also contains a P-type, Type  
24 IV secretion system (T4SS) supporting self-transfer to other *P. putida* strains. This study increases our  
25 understanding in the build-up of IncP-2 plasmids and several promising exchangeable gene clusters to  
26 construct robust microbial hosts for biotechnology applications.

## 27 **Importance**

28           Originating from various environmental niches, large numbers of bacterial plasmids have been  
29 found carrying heavy metal and antibiotic resistance genes, degradation pathways and specific  
30 transporters for organic solvents or aromatic compounds. Such genes may constitute promising  
31 candidates for novel synthetic biology applications. Our systematic analysis of gene clusters encoded  
32 on megaplasmid pTTS12 underscores that a large portion of its genes is involved in stress response  
33 increasing survival under harsh conditions like heavy metal and organic solvent resistance. We show  
34 that pTTS12 belongs to the IncP-2 plasmid family. Comparative analysis of pTTS12 provides thorough  
35 insight into the structural and functional build-up of members of the IncP-2 plasmid family. pTTS12 is  
36 highly stable and carries a complex arrangement of transposable elements containing heavy metal  
37 resistance clusters as well as distinct aromatic degradation pathways and solvent-extrusion pump.  
38 This offers interesting insight into the evolution of solvent tolerance in the *P. putida* family.

39

## 40 **Introduction**

### 41 **Megaplastids as transferable vehicles of environmental resistance genes**

42 Bacteria may use plasmids as autonomous, self-replicating elements driving horizontal transfer of  
43 genes (HGT) that confer resistance to otherwise detrimental conditions. As such, these  
44 extrachromosomal entities often confer advantageous characteristics for the host strain (1–3). The  
45 rapid spread of resistance genes through these, usually large conjugative plasmids is further facilitated  
46 by the presence of a variety of mobile genetic elements such as transposons, integrons and insertion  
47 sequences (IS's) (4–7). The spread of multidrug resistance (MDR) via mobile genetic elements has  
48 been the subject of investigation for a number of years (8). Despite those efforts, the role and  
49 functioning of megaplastids is still poorly understood. Recent studies highlighted the role of  
50 megaplastids in the spread of MDR in the opportunistic pathogen *Pseudomonas aeruginosa* (1, 2).  
51 Strains of its close relative, *Pseudomonas putida*, have been known to harbor large conjugational  
52 plasmids, conferring resistance to environmental threats (3, 9). Plasmids of the *Pseudomonas* family  
53 are classified by incompatibility groups, that exhibit various modes of compatibility and transferability  
54 (10). We have chosen to study the recently identified megaplastid pTTS12 of *Pseudomonas putida*  
55 S12 in comparison with a number of other large plasmids of the *Pseudomonas* family, in order to  
56 elucidate key elements governing HGT, stability and essential functions.

57

### 58 **Solvent tolerance in *Pseudomonas putida* S12; resistance as a benefit for biotechnology**

59 *Pseudomonas putida* S12 is a gram-negative soil bacterium which was isolated on styrene as a sole  
60 carbon source (11). This strain shows a remarkable tolerance towards non-metabolized organic  
61 solvents (e.g. toluene) (12). Such high tolerance towards organic solvents presents a beneficial trait  
62 and advantage for bioproduction of aromatics and biofuel (13, 14). Due to its solvent tolerance and  
63 versatile metabolism, *P. putida* S12 excels as a microbial host for production of valuable chemicals  
64 (15–19). Removal of organic solvent molecules from the bacterial cell membrane is essential and  
65 carried out by SrpABC, a resistance-nodulation-cell division (RND) family efflux pump (12, 20).

66 Membrane compaction and the upregulation of chaperones, general stress responses, and TCA cycle-  
67 related enzymes support a further intrinsic solvent tolerance in *P. putida* S12 (21–24).

68 We recently found through whole-genome sequencing that the genome of *P. putida* S12  
69 consists of a 5.8 Mbp chromosome and a 583 kbp single-copy megaplasmid pTTS12 (25). Interestingly,  
70 both the SrpABC RND-efflux pump and the styrene degradation pathway which are major distinctive  
71 features of *P. putida* S12, are encoded on this megaplasmid. The genome of *P. putida* S12 contains a  
72 large number of several types of mobile elements, spread over both chromosome and megaplasmid  
73 pTTS12 (25–27). Some of these insertion sequences were shown to be involved in the regulation and  
74 adaptation towards stress conditions, for example during the solvent stress (4, 28). Like *P. putida* S12,  
75 related solvent-tolerant *P. putida* DOT-T1E and *Pseudomonas taiwanensis* VLB120 have been shown  
76 to harbor megaplasmids of 121 kb and 312 kb, respectively (29, 30). Indeed, those plasmids encode  
77 RND-type efflux pumps and biodegradative pathways for aromatic compounds, similar to *P. putida*  
78 S12. To further characterize pTTS12, we here performed a comparative analysis against a large  
79 number of other megaplasmids from Refseq and Nuccore databases. With this analysis, we aimed at  
80 identifying the origin of the pTTS12 plasmid and understanding the build-up of environmental-stress  
81 related gene clusters in pTTS12.

82

83

## 84 Results

### 85 Comparative analysis of megaplasmid pTTS12

86 The 583 Kbps megaplasmid pTTS12 (GenBank accession no. CP009975) is a single-copy plasmid  
87 encoded in *P. putida* S12 (25). For this paper, annotations for pTTS12 were further extended (Table  
88 S1) and the overall sequence was corrected based on our previous observations of an additional seven  
89 ISS12 mobile elements (4). pTTS12 encodes 609 genes of which 583 are single copy and 15 genes are  
90 duplicated at least once. These genes were divided into 232 putative operons for subsequent ordered  
91 genes in forward or reverse strand with less than 20 bps distance. The operons were clustered  
92 together based on the function of genes encoded within these clusters (Table S1).

93 Comparative analysis was performed with 28915 plasmids larger than 2 kb in length, acquired  
94 from the Refseq database (<https://www.ncbi.nlm.nih.gov/refseq/>) combined with additional  
95 sequences from the Nuccore database (<https://www.ncbi.nlm.nih.gov/nuccore/>). The top 50 plasmids  
96 encoding homologues of pTTS12 proteins are visualized in a circular plot using CGView (31) as shown  
97 on Figure 1, and listed in Table 1. In Figure 1, the outer purple line represents pTTS12 with forward  
98 coding genes on top of the line and the reverse coding gene sequences below the line. Each of the  
99 subsequent 50 inner circles represents a single plasmid and is colored based on the family of its host.  
100 In case no homologous protein was identified for a pTTS12 counterpart, that space on the circle was  
101 left blank. The extended circular plot and list of the top 500 plasmids encoding homologues of pTTS12  
102 can be found in Figure S1 and Table S2.

103 The majority of plasmids highly similar to pTTS12 were found in *Pseudomonas* type strains  
104 (Table 1). The relative identity scores presented in Table 1 were calculated as a percentage of total  
105 scores of each plasmid divided by the total identity score obtained for pTTS12 itself. The plasmid most  
106 similar to pTTS12 is pOZ176 from *P. aeruginosa* PA96 which was previously categorized as a member  
107 of incompatibility group P-2 (IncP-2). pOZ176 and pTTS12 share no less than 71% similarity of their  
108 encoded genes indicating that these plasmids share a similar IncP-2 backbone. However, while

109 pOZ176 encodes a carbapenem-resistance gene cluster typical for several pathogenic *P. aeruginosa*  
110 strains (2), pTTS12 of *P. putida* S12 does not share this feature.

111 Surprisingly, pTTS12 shares only 21% of sequence similarity with the pSTY plasmid of *P.*  
112 *taiwanensis* VLB120. The major and only gene clusters shared between pTTS12 and pSTY are involved  
113 in styrene degradation, phenylpropionic acid degradation, and solvent efflux pump (SrpABC).  
114 Interestingly, the genes shared between pTTS12 and pSTY are absent in all other *Pseudomonas*  
115 plasmids, except for the solvent efflux pump gene cluster which is similar with TtgGHI efflux pump  
116 from the pGRT-1 plasmid of *P. putida* DOT-T1E. The regions encoding solvent efflux pump and  
117 phenylpropionic acid degradation are clustered together and have identical synteny in pTTS12 and  
118 pSTY (Figure S2). However, the plasmids do not share any mobile genetic elements surrounding this  
119 cluster that might indicate a mechanism of acquisition or transfer. The similarity of the styrene  
120 degradation clusters and solvent efflux pump - phenylpropionic acid degradation clusters between  
121 pTTS12 and pSTY were 99% and 80%, respectively.

122 Between 8% to 12% of encoded proteins from pTTS12 can also be found in other genera than  
123 *Pseudomonas* (Table 1). Several plasmids from *Salmonella*, *Enterobacter*, *Citrobacter*, *Leclersia*,  
124 *Klebsiella*, *Pantoea*, *Polaromonas*, and *Cupriavidus* species shared homologous proteins involved in  
125 the T4SS conjugation, replication machinery, and plasmid maintenance. Like other IncP-2 plasmids,  
126 pTTS12 contains multiple transposable elements, particularly Tn3 mobile elements (Figure 1). This  
127 mobile element encodes for heavy metal resistance genes that are predominantly present in IncP-2  
128 plasmids. Additionally, pTTS12 carries a unique Tn7-element consisting of several chromate resistance  
129 genes.

130

### 131 **Distinctive conjugation machinery of pTTS12**

132 Megaplasmid pTTS12 contains a P-type T4SS (Type IV secretion system) conjugation system  
133 (RPPX\_28670-RPPX\_28725), sharing synteny with the prototype *trb* operon from *A. tumefaciens*  
134 pTiC58 (Figure 2A). For an operational T4SS conjugation machinery, a T4SS gene cluster, type IV  
135 coupling protein (T4CP) and a relaxase protein are required (32). An additional *traG* (RPPX\_28650),

136 which may serve as a T4CP, is located upstream of the T4SS cluster. Further upstream of the T4SS and  
137 T4CP, a putative virD2-like gene (RPPX\_28750) and an operon consisting of *parB*, *parA* and *repA*  
138 (RPPX\_28765-28775) are encoded on pTTS12. The putative virD2-like gene (RPPX\_28750) may play a  
139 role as a relaxase which is important for the transferability of pTTS12.

140 T4SS, *traG*, and upstream genes involved in replication and partitioning shared synteny with  
141 the T4SS clusters on other plasmids such as *Pantoea sp.* PSNIH1 (pPSP-a3e), *Pseudomonas aeruginosa*  
142 PA96 (pOZ1760), and *Ketogulonicigenium vulgare* SKV (pKvSKV1) (Figure 2B). Typically, *traG* (T4CP) is  
143 coupled to the same operon of T4SS while the region encoding replication and partitioning may be  
144 separated (Figure 2B), in some cases relatively far. It is interesting to note that in two *Mesorhizobium*  
145 *loti* strains and *Novosphingobium sp.* PP1Y, the T4SS operon and *traG-tral* are completely separated  
146 (Figure 2B). Instead, VirD2-like protein (relaxase), *traG* (T4CP) and *tral* formed a single operon.

147 Most of the Pseudomonadaceae-family plasmids do not contain this *trb* operon (Figure 1)  
148 except for pTTS12, pOZ176 from *P. aeruginosa* PA96, pJB37 from *P. aeruginosa* FFUP\_PS\_37 and an  
149 unnamed plasmid from *P. aeruginosa* PA83. Therefore, this conjugative operon may not be common  
150 in IncP-2 plasmid family. However, this *trb* operon is abundant among Enterobacteriaceae-family  
151 plasmids (Figure 1).

152

### 153 **Distribution of transposable elements conferring heavy metal resistance**

154 pTTS12 as well as many other highly similar plasmids contain a multitude of mobile genetic elements,  
155 such as ISS12 and Tn3-family transposases. pTTS12 harbors five copies of Tn3-family transposable  
156 elements; two copies of Tn3-I with highest identity to Tn4656, two copies of Tn3-II that are highly  
157 similar to Tn5053 and a single copy of Tn3-III with highest similarity to Tn5563 (Figure 3A). Tn3-I is an  
158 identical transposase (RPPX\_RS27515, *tnpR* and RPPX\_RS27515, *tnpA*) to Tn4656 encoded on pWW53  
159 plasmid from *P. putida* MT53. Moreover, the 39-bps inverted repeat (IR) sequences found on both  
160 ends of these two elements are highly identical with only a single mismatch difference. In addition to  
161 *tnpA* and *tnpR*, this Tn3-element contains a putative methyl-accepting chemotaxis protein (*mcpT-2*)  
162 and an insertion sequence IS256. Tn3-II of pTTS12 is identical (99.8% similarity) to Tn5053 of

163 *Xanthomonas* sp. W17 encoding a mercury resistance gene cluster *merR* and *merTPAD* (7). This Tn3-II  
164 has 25 bp inverted repeats, bracketing the ends and 5 bp directed repeats (DR). Tn3-III is identical to  
165 Tn5563, that is found in several other plasmids, eg. pAMBL of *P. aeruginosa*, pSTY of *P. taiwanensis*  
166 VLB-120 and pRA2 of *P. alcaligenes*. The Tn3-III has identical 38 bps IRs bracketing the element, also  
167 identical to IRs found for this element in other plasmids. This element contains several genes such as  
168 *merR*, *merTP*, *pilT* and a gene with a PIN nuclease domain.

169 The Tn4656 and Tn5563 are both duplicated and rearranged on the megaplasmid together  
170 with Tn5053. This rearrangement resulted in a highly characteristic sequence, which partially resulted  
171 from insertion of Tn5053 transposition in the second copy of Tn4656 (Tn4656-II), between the *mcpT*-  
172 2 and *tnpR* loci (Figure 3). The IRs as well as DRs of Tn5053 indicate the insertion site of this element.  
173 The IRs of Tn4656-II are well preserved bracketing both elements. Other parts of this sequence consist  
174 of the second copy of Tn5563 (Tn5563-II), which is truncated at the right end by insertion of Tn4656-  
175 II in *merT* and thus truncated the 5' end of *merT* sequence, can be identified. Due to this truncation,  
176 the IRs of Tn4656-II cannot be found on the right side of the element anymore except for the right IR  
177 of initial Tn4656, which is located 58 kbps upstream of this element.

178 The unique rearrangement of the three different Tn3 elements in pTTS12 surprisingly is also  
179 present on pSTY of *P. taiwanensis* VLB120, including an additional copy of Tn5563. In between these  
180 two Tn5563-elements, both megaplasmids contain the complete styrene degradation pathway,  
181 enabling both strains to grow on styrene as sole carbon source (25, 30). Detailed comparison of the  
182 regions between the two Tn5563 elements from pTTS12 and pSTY reveals a high similarity between  
183 Tn5563-I and Tn5563-II (Figure 3B). This sequence is around 77 kbps and 60 kbps for pTTS12 and pSTY  
184 respectively, including the IRs bracketing both sequences.

185 In addition to Tn3-elements, a unique Tn7-like element (20 kbps) is also encoded on pTTS12  
186 (Figure 1). Interestingly, an identical transposable element is also encoded on the chromosome of *P.*  
187 *putida* S12. This element contains several transposase genes at both ends and a putative chromate  
188 resistance gene cluster (locus tag RPPX\_28930-29030; see Table S1). The putative chromate resistance  
189 gene cluster was identified based on homology search using BLAST and alignments to other plasmids.



190 RPPX\_28995, RPPX\_28990, and RPPX\_29000 were identified to encode for a chromate resistance  
191 efflux pump ChrA, and two regulatory proteins ChrB and ChrF respectively similar to the chromate  
192 resistance gene cluster carried by pMOL28 of *Cupriavidus metallidurans* CH34 (33).

### 193 **Conjugative megaplasmid pTTS12 is highly stable in *P. putida* KT2440**

194 To characterize the conjugative transferability of pTTS12, we performed biparental mating between  
195 *P. putida* S12.1 and *P. putida* KT-BG35. *P. putida* KT-BG35 is a strain derived from *P. putida* KT2440,  
196 does not harbour a megaplasmid and carries a gentamicin resistant marker and green fluorescence  
197 protein (GFP) at its *atn7* site (34). The transfer was performed using biparental mating between *P.*  
198 *putida* S12.1 containing pTTS12 with kanamycin resistant marker and *P. putida* KT-BG35.  
199 Transconjugant colonies resistant to both kanamycin and gentamicin occurred at the frequency of  
200  $4.20 (\pm 0.51) \times 10^{-7}$ . After appropriate selection on agar plates, the identity of transconjugant colonies  
201 was confirmed by observing GFP expression of the colonies derived from *P. putida* KT-BG35.  
202 Additionally, transfer of entire pTTS12 was confirmed using PCR. Amplification of several regions of  
203 pTTS12 using primer pairs 53,496\_Fw-56,596\_Rv, 200,497\_Fw-203,602\_Rv, and 286,448\_Fw-  
204 289,462\_Rv resulted in an expected band of 3 kbp in transconjugant colonies. All 15 randomly selected  
205 colonies chosen for colony PCR showed correct bands. This confirmed the transfer of entire pTTS12  
206 into *P. putida* KT-BG35 and the resulting strains will further be referred to as *P. putida* KTpS12. Several  
207 attempts to transfer pTTS12 into *E. coli* strains represented by *E. coli* MV1190 and *E. coli* XL1-Blue by  
208 biparental mating did not result in any successful transconjugant colonies.

209 The putative relaxase gene, *virD2*, was identified on pTTS12 (locus tag RPPX\_28750). To  
210 confirm this finding, we created a complete deletion of *virD2* gene and compared the self-transfer  
211 frequency of pTTS12  $\Delta virD2$  and wild-type pTTS12 into *P. putida* KT2440. The transfer frequency of  
212 pTTS12  $\Delta virD2$  was  $4.16 (\pm 0.08) \times 10^{-7}$ , which was not significantly different (p-value 0.8867)  
213 compared to the transferability of the wild-type pTTS12 from *P. putida* S12 to *P. putida* KT2440.

214 The stability of pTTS12 in *P. putida* KTpS12 and *P. putida* S12 was examined for 5 passages in  
215 the absence of antibiotic selective pressure (approximately 10 generations/passage step). No plasmid

216 loss was observed from either *P. putida* KTpS12 or *P. putida* S12 growing without selective pressure  
217 while the negative control pSW-2 showed a steady plasmid loss (Figure 4A). Serendipitous deletion of  
218 pTTS12 was not found in *P. putida* S12 and *P. putida* KTpS12 either. Hence, pTTS12 is a stable  
219 megaplasmid in both *P. putida* S12 and *P. putida* KT2440.

220 The occurrence of large plasmids in bacteria is known to cause metabolic burden, which is  
221 reflected in reduced bacterial growth rate ( $\mu$ ). *P. putida* KTpS12 exhibited a lower maximum growth  
222 rate compared to *P. putida* KT2440,  $0.686 \pm 0.012$  and  $0.856 \pm 0.021$  h<sup>-1</sup> respectively (Figure 4B).  
223 However, *P. putida* S12 and *P. putida* S12  $\Delta$ pTTS12 did not show a significant maximum growth rate  
224 difference ( $0.713 \pm 0.009$  and  $0.659 \pm 0.030$  h<sup>-1</sup> respectively). The length of lag-phase and biomass  
225 yield at stationary phase remained unaffected with pTTS12 present in both *P. putida* S12 and KTpS12.  
226 Apparently, the presence pTTS12 imposes a only slight metabolic burden in *P. putida* KT2440, but not  
227 in S12.

228

#### 229 **Phenotypic features of pTTS12 and attained solvent tolerance in *P. putida* KT2440**

230 *P. putida* S12 is intrinsically tolerant to an assortment of environmental xenobiotics. The majority of  
231 these characteristic traits are encoded on pTTS12; the styrene degradation operon *styABCDE*, the  
232 tellurite resistance operon *terZABCDE* and a solvent efflux pump *srpABC*. To explore functionality of  
233 pTTS12 following conjugative transfer, these characteristic traits were investigated in *P. putida* KTpS12  
234 (Figure 5). Activity of the styrene degradation operon in *P. putida* KTpS12 was tested by growing on  
235 minimal media with styrene as carbon source and inspecting transformation of indole into indigo.  
236 Similarly as observed in *P. putida* S12, *P. putida* KTpS12 was able to transform indole into indigo,  
237 whereas wild-type KT2440 was not, indicating activity of styrene monooxygenase (*styA*) and styrene  
238 oxide isomerase (*styB*) in these strains (Figure 5A). In addition, *P. putida* KTpS12 was able to grow on  
239 minimal media supplemented with styrene as carbon source or minimal media agar plates incubated  
240 in styrene atmosphere (data not shown).

241 Potassium tellurite (K<sub>2</sub>TeO<sub>3</sub>) exhibits antimicrobial activity and tellurite resistance in bacteria  
242 is achieved through reduction of tellurite (TeO<sub>3</sub><sup>2-</sup>) into a less toxic metallic tellurium (Te<sup>0</sup>), hence the

243 formation of black colonies in the presence of tellurite (35). The resistance genes on pTTS12 are  
244 encoded as an operon *terZABCDE* (RPPX\_26360-26385). To investigate whether this gene cluster is  
245 able to increase resistance towards tellurite in *P. putida* KT2440, the minimum inhibitory  
246 concentration (MIC) was determined for the three different stains (Figure 5B). The MIC of potassium  
247 tellurite for *P. putida* KT2440 was 16 fold less compared to *P. putida* S12, 12.5 mg L<sup>-1</sup> and 200 mg L<sup>-1</sup>  
248 respectively. Interestingly, *P. putida* KTpS12 showed an 8 fold increase in tellurite resistance (MIC 100  
249 mg L<sup>-1</sup>) compared to its parental strain *P. putida* KT2440.

250           The solvent efflux pump *srpABC* encoded on the megaplasmid pTTS12, enables survival and  
251 growth of *P. putida* S12 in non-utilized organic solvents (36). In order to investigate the effect of  
252 induced tolerance toward organic solvents due to the introduction of pTTS12 in *P. putida* KTpS12, a  
253 growth assay was performed in the presence of different toluene concentrations (Figure 5C). *P. putida*  
254 KT2440 was able to grow in LB liquid media supplemented with toluene up to a maximum of 0.15 %  
255 v/v concentration, although suffering from a significant growth reduction compared to *P. putida* S12.  
256 With the introduction of pTTS12, *P. putida* KTpS12 tolerance toward toluene increased to 0.30 % v/v.  
257 Similar concentration was obtained for *P. putida* S12, while *P. putida* KTpS12 exhibited slightly slower  
258 growth in the presence of toluene. These observations indicated that the introduction of megaplasmid  
259 pTTS12 provided a full set of characteristic features to *P. putida* KT2440.

260

## 261 Discussion

### 262 Megaplasmid pTTS12 defines an environment-adaptive and type-specific family of IncP-2 plasmids, 263 carrying distinct accessory gene clusters

264 Megaplasmid pTTS12 of *P. putida* S12 is closely related to other plasmids in proteobacteria, especially  
265 within the *Pseudomonas* genus. In this study we demonstrated high similarity of the pTTS12  
266 'backbone' with pOZ176 from *P. aeruginosa* PA96 (2) and several other IncP-2 plasmids, such as  
267 pQBR103 of *Pseudomonas fluorescens* SBW25 (37). pOZ176 has been categorized within  
268 incompatibility group IncP-2 based on its replication, partitioning, and transfer machinery along with  
269 conferring tellurite resistance as a key feature of IncP-2 plasmid (2, 5). Indeed, pTTS12 encodes typical  
270 characteristics of IncP-2 plasmids, such as heavy metal resistance (tellurite, mercury, and chromate)  
271 and plasmid maintenance via the *parA/parB/repA* system (10, 38). pTTS12 clearly conferred tellurite  
272 resistance when transferred to tellurite-susceptible *P. putida* KT2440, confirming this IncP-2  
273 characteristic phenotype. Interestingly, despite high similarity between pTTS12 and pOZ176, pTTS12  
274 lacks the Tn6016 *bla*<sub>IMP-9</sub>-carrying class 1 integron cassette which is an important trait of pOZ176  
275 conferring resistance to aminoglycosides and carbapenems (2, 5). On the other hand, pOZ176 lacks  
276 the solvent efflux pump, styrene degradation pathway, and phenylpropionic acid degradation  
277 pathway which are main characteristics of pTTS12. This demonstrates that very similar megaplasmid  
278 backbones may carry resistance to a diversity of xenobiotics, metabolic functions, or virulence gene  
279 clusters (39). Whereas the traits disseminated by pTTS12 and pOZ176 respectively, are highly  
280 divergent and distinctive, a similar observation of environment-adaptive traits conferred by flexible  
281 and diverse accessory gene clusters contained on IncP-2 plasmids was recently reported for *P.*  
282 *aeruginosa* plasmids pBT2436 and pBT2101, carrying multiple MDR cassettes (1).

283

### 284 Convergent distribution of plasmid-encoded solvent tolerance gene clusters

285 pTTS12 shares its unique features of styrene and phenyl-propanoate degradation pathway with *P.*  
286 *taiwanensis* VLB120 and the solvent extrusion pump SrpABC with TtgGHI from *P. taiwanensis* VLB120  
287 and *P. putida* DOT-T1E. These solvent tolerant strains were isolated independent of each other,

288 although in different geographical locations; *P. putida* S12 and *P. taiwanensis* VLB120 were isolated  
289 for their ability to utilize styrene as sole carbon source (11, 40). *P. putida* DOT-T1E was isolated for its  
290 ability to degrade toluene (9). Hence, these plasmids isolated from different environmental sources  
291 show convergent distribution of highly similar gene clusters with similar features related to  
292 environmental stresses (e.g. organic solvents) on different plasmid backbones. In *P. taiwanensis*  
293 VLB120, the arrangement of gene clusters encoding the styrene degradation pathway and solvent  
294 efflux pump - phenylpropionic acid degradation pathway is highly similar to pTTS12, with 99% and  
295 80% similarity, respectively. This moreover, indicates that exchange of the styrene degradation  
296 pathway occurred more recently than exchange of the efflux pump/phenylpropionic acid degradation  
297 cluster. Alternatively, these clusters may have been acquired independently.

298 The styrene degradation gene cluster is encoded within a unique arrangement of Tn3 family  
299 transposases shared by pTTS12 and pSTY from *P. taiwanensis* VLB120 (Figure 3). Due to the  
300 transposition of Tn3-Ib, Tn3-IIa lost its right flank inverted repeat (IR). Because of this arrangement,  
301 Tn3-IIa can only “jump” while carrying the entire Tn3 and styrene-phenylacetate degradation clusters  
302 using the right flank of Tn3-IIb IR. This may explain the occurrence of the styrene-phenylacetate  
303 degradation cluster distinctive arrangement shared between pTTS12 and pSTY. Although we could not  
304 find evidence of mobile genetic elements carrying the efflux pump and the phenylpropionic acid  
305 degradation gene clusters on pSTY and pTTS12, it is well possible that the exchange originally occurred  
306 via such route.

307

### 308 **Transferability of pTTS12**

309 pTTS12 contains a P-Type type IV secretion system (T4SS) with synteny similar to the prototype *trb*  
310 operon of the *A. tumefaciens* pTiC58 system (32, 41). Indeed, our experiments showed that pTTS12 is  
311 transferable towards other *P. putida* strains with a frequency of  $4.20 (\pm 0.51) \times 10^{-7}$ . A putative  
312 relaxase, responsible for creating a nick prior to plasmid transfer via the conjugative bridge, was  
313 predicted to be encoded by *virD2* (locus tag RPPX\_28750). However, complete deletion of *virD2* did  
314 not result in a significant reduction of transfer frequency, compared to the wild-type pTTS12. This

315 may indicate the presence of other relaxase(s) which act in-trans with the P-type T4SS to mediate the  
316 nicking of plasmid DNA and subsequently aided the plasmid transfer process. *P. putida* S12 contains  
317 other T4SS within its genome which share synteny with the I-type T4SS represented by Dot/Icm from  
318 *L. pneumophila* (Figure S3), although it is unclear whether Dot/Icm can support the transfer of pTTS12  
319 (42).

320

### 321 **Amelioration of pTTS12 reduces fitness cost and promotes plasmid persistence in *P. putida* S12**

322 We observed that in its original host *P. putida* S12 on rich media, pTTS12 did not impose an apparent  
323 metabolic burden whereas in another strain as *P. putida* KT2440, pTTS12 caused a 20% reduction of  
324 maximum growth rate. We previously reported on the occurrence of metabolic burden caused by  
325 pTTS12 in *P. putida* S12 in the presence of toluene (43). In addition to the relatively low metabolic  
326 burden, pTTS12 was very stable in both *P. putida* S12 and *P. putida* KT2440 (Figure 4A). Several  
327 mechanisms may be involved in the reduced fitness cost and the stability of pTTS12 in *P. putida* S12.

328 Conjugative transfer may impose substantial cost and burden due to the energy investment  
329 on pili formation during conjugation (39, 44). Indeed, pTTS12 showed a substantially lower  
330 conjugation rate ( $4.20 \times 10^{-7}$  transfer frequency) after 24 hours in comparison to other IncP-2 plasmids  
331 ( $10^{-1}$  to  $10^{-4}$  transfer frequency after 2 hours) (38). Downregulation of plasmid genes appeared to be  
332 involved in the amelioration of pTTS12. The expression of plasmid-encoded resistance genes, like the  
333 solvent extrusion pump, can typically be a source of metabolic burden imposed by plasmids (45).  
334 pTTS12 contains multiple types of mobile genetic elements, with ISS12 being the most abundant (4,  
335 27). Substantial duplication of the ISS12 mobile element has previously been reported to interrupt  
336 *srpA*, encoding the periplasmic subunit of the solvent efflux pump (4). In the prolonged absence of  
337 organic solvent, expression and maintenance of the solvent efflux pump may be costly for the bacterial  
338 cell, hence, interruption of the *srp* efflux pump gene cluster may further reduce the plasmid burden  
339 of pTTS12. In addition to these mechanisms, we recently described the contribution of a toxin-  
340 antitoxin module SlvT-SlvA to the stability of pTTS12 (43).

341

## 342 **Future outlook**

343 IncP-2 family plasmids are widely distributed among environmental and clinical *Pseudomonas* isolates.  
344 These plasmids contain variable regions encoding MDR, xenobiotics extrusion pumps, degradation  
345 pathways, and heavy metal resistance cassettes. In contrast to the dynamic variable regions, the core  
346 backbone of these plasmids shows a general conservation. It is interesting to discover the minimal  
347 backbone of IncP-2, which enables *Pseudomonads* to scavenge gene clusters important for its survival  
348 both in environmental and clinical set-up, as a model of horizontal gene transfer. Ultimately, IncP-2  
349 plasmid backbone may be promising for biotechnological and bioremediation applications due to its  
350 stability and relatively low metabolic burden. Moreover, these plasmids have been described to  
351 exchange their traits, thus creating hybrid plasmids when they occur within the same host (38). The  
352 mechanisms for such exchange are poorly understood and may well involve transposition and  
353 conjugation as suggested by the shared and type-specific characteristics of pTTS12 and pOZ176 as  
354 described in this study. Further clarification of these mechanisms is important to shed light on the  
355 rapid dissemination of bacterial tolerance and resistance to antibiotics and chemical stresses in the  
356 environment.

357         Successful attempts have been made in exploiting traits from environmental plasmids for  
358 standardized components in synthetic biology (46). Environmental plasmids are exchangeable  
359 between different hosts and may express their genetic features in various genomic and metabolic  
360 backgrounds. Moreover, they are an excellent source of novel biological parts such as origin of  
361 replication, metabolic pathway, resistance marker, and regulated promoters. New sequencing  
362 technologies and comparative genomics analyses support the identification of the genes enabling  
363 these features. Here, we demonstrated that pTTS12 contains promising exchangeable gene clusters  
364 and building blocks to construct robust microbial hosts for high-value biotechnology applications.

365

366

367

## 368 **Materials and methods**

### 369 **Cultivation of *P. putida***

370 Strains and plasmids used in this report were listed in Table 2. All *P. putida* strains were grown in  
371 Lysogeny Broth (LB) containing 10 g L<sup>-1</sup> tryptone, 5 g L<sup>-1</sup> yeast extract and 5 g L<sup>-1</sup> sodium chloride at 30  
372 °C with 200 rpm shaking. *E. coli* strains were cultivated in LB at 37 °C with 250 rpm shaking in a  
373 horizontal shaker (Innova 4330, New Brunswick Scientific). For solid cultivation, 1.5 % (w/v) agar was  
374 added to LB. M9 minimal medium used in this report was supplemented with 2 mg L<sup>-1</sup> MgSO<sub>4</sub> and 0.2%  
375 w/v of citrate as sole carbon source (11). Bacterial growth was observed by optical density  
376 measurement at 600 nm (OD<sub>600nm</sub>) using a spectrophotometer (Ultrospec 2100 pro, Amersham  
377 Biosciences). Maximum growth rate and other parameters were calculated using growthcurver R-  
378 package ver.0.3.0 (47). Solvent tolerance analysis was performed by growing *P. putida* strains in LB  
379 starting from OD<sub>600nm</sub> = 0.1 in Boston bottles with Mininert bottle caps. When required, potassium  
380 tellurite (6.75 - 200 mg L<sup>-1</sup>), indole (100 mg L<sup>-1</sup>), gentamicin (25 mg L<sup>-1</sup>), ampicillin (100 mg L<sup>-1</sup>),  
381 tetracycline (25 mg L<sup>-1</sup>), and kanamycin (50 mg L<sup>-1</sup>) were added to the media.

382

### 383 **DNA methods**

384 All PCR reaction were performed using Phire polymerase (Thermo Fischer) according to the  
385 manufacturer's manual. All primers are listed in Table 3 and were obtained from Sigma-Aldrich. PCR  
386 reactions were visualized and analyzed by gel electrophoresis on 1 % (w/v) TBE agarose gels containing  
387 5 mg L<sup>-1</sup> ethidium bromide in an electric field (110V, 0.5x TBE running buffer).

388

### 389 **Megaplasmid pTTS12 transfer into *P. putida* KT2440 and *E. coli* strains**

390 Gentamicin resistance and GFP containing cassette were incorporated into *P. putida* KT2440  
391 chromosome at the Tn7 site using pBG35 plasmid resulting in the strain *P. putida* KT-BG35 as  
392 previously described (34). Correct transformants were additionally verified by observing the  
393 gentamicin resistance, GFP expression and colony PCR of *P. putida* KT2440 chromosome sequence.



394 Kanamycin resistance gene was introduced into the megaplasmid pTTS12 by integrating plasmid  
395 pEMG using homologous recombination resulting in *P. putida* S12.1 as previously described (48). A  
396 single homologous recombination site was obtained by PCR with 90285\_Fw and 90825\_Rv primer pair  
397 and this fragment was used to construct pEMG-TS plasmid. Correct integration into *P. putida* S12 was  
398 verified by observing kanamycin resistance and colony PCR using primers 4,963,661\_Fw-  
399 4,966,726\_Rv.

400 The transfer of pTTS12 into *P. putida* KT-BG35, *E. coli* XL1-Blue or *E. coli* MV1190 were performed by  
401 biparental mating between *P. putida* S12.1 and the recipient strain on LB agar for 24 hours at 30 °C.  
402 The correct transformants were selected using LB agar supplemented with gentamicin and kanamycin  
403 for *P. putida* KT-BG35 or with tetracycline and kanamycin for *E. coli* strains. Additionally, transformants  
404 were verified using colony PCR (53,496\_Fw-56,596\_Rv, 200,497\_Fw-203,602\_Rv, and 286,448\_Fw-  
405 289,462\_Rv). Plasmid transfer rate was determined by comparing the event of successful plasmid  
406 transconjugant with the colony formation unit (cfu) of the recipient strain (*P. putida* KT-BG35, *E. coli*  
407 XL1-Blue or *E. coli* MV1190) after biparental mating ( $Gm^R/Tc^R$ ). Plasmid stability was determined by  
408 calculating the event of megaplasmid loss in *P. putida* KTpS12 grown in liquid media without  
409 supplementation of kanamycin as the selective pressure for pTTS12. Plasmid pSW-2 was used as a  
410 control for megaplasmid loss events (48).

411

## 412 **Sequence analyses**

413 All plasmid sequences were downloaded from NCBI database, 22389 plasmid sequences from Refseq  
414 database (retrieved 8 March 2020) and complemented with few plasmid sequences from NUCORE  
415 that were omitted from Refseq. The CGviewer (31) was used to generate circular plots of entire  
416 pTTS12 with standard settings and MultiGeneBlast tool (49) was used to generate synteny plots of  
417 specific regions and operons. Further analysis was performed using Geneious software (BioMatters),  
418 and selected sequences were aligned using MAFFT (50) for DNA sequences or MUSCLE (51) for protein  
419 sequences.

420

421 **Acknowledgement**

422 We thank Erik Vijgenboom and Gerben Voshol (Leiden University) for helpful discussions and Omar  
423 Qachach for his assistance during the data acquisition process. R. Hosseini was funded by the Dutch  
424 National Organization for Scientific Research NWO, through the ERAnet-Industrial Biotechnology  
425 programme, project “Pseudomonas 2.0”. H. Kusumawardhani was supported by the Indonesia  
426 Endowment Fund for Education (LPDP) as scholarship provider from the Ministry of Finance,  
427 Indonesia.

428

429

## 430 References

- 431 1. Cazares A, Moore MP, Hall JPJ, Wright LL, Grimes M, Emond-Rhéault JG, Pongchaikul P,  
432 Santanirand P, Levesque RC, Fothergill JL, Winstanley C. 2020. A megaplasmid family driving  
433 dissemination of multidrug resistance in *Pseudomonas*. *Nat Commun* 11:1370.
- 434 2. Xiong J, Alexander DC, Ma JH, Déraspe M, Low DE, Jamieson FB, Roy PH. 2013. Complete  
435 Sequence of pOZ176, a 500-Kilobase IncP-2 Plasmid Encoding IMP-9-Mediated Carbapenem  
436 Resistance, from Outbreak Isolate *Pseudomonas aeruginosa* 96. *Antimicrob Agents Chemother*  
437 57:3775–3782.
- 438 3. Molina L, Duque E, Gómez MJ, Krell T, Lacal J, García Puente A, García V, Matilla MA, Ramos J-  
439 L, Segura A. 2011. The pGRT1 plasmid of *Pseudomonas putida* DOT-T1E encodes functions  
440 relevant for survival under harsh conditions in the environment. *Environ Microbiol* 13:2315–  
441 2327.
- 442 4. Hosseini R, Kuepper J, Koebbing S, Blank LM, Wierckx N, de Winde JH. 2017. Regulation of  
443 solvent tolerance in *Pseudomonas putida* S12 mediated by mobile elements. *Microb*  
444 *Biotechnol* 10:1558–1568.
- 445 5. Xiong J, Hynes MF, Ye H, Chen H, Yang Y, M’Zali F, Hawkey PM. 2006. *bla*<sub>IMP-9</sub> and its association  
446 with large plasmids carried by *Pseudomonas aeruginosa* isolates from the People’s Republic of  
447 China. *Antimicrob Agents Chemother*.
- 448 6. Nojiri H, Shintani M, Omori T. 2004. Divergence of mobile genetic elements involved in the  
449 distribution of xenobiotic-catabolic capacity. *Appl Microbiol Biotechnol* 64:154–174.
- 450 7. Kholodii GY, Yurieva O V., Lomovskaya OL, Gorlenko ZM, Mindlin SZ, Nikiforov VG. 1993.  
451 Tn5053, a mercury resistance transposon with integron’s ends. *J Mol Biol* 230:1103–1107.
- 452 8. Partridge SR, Kwong SM, Firth N, Jensen SO. 2018. Mobile genetic elements associated with  
453 antimicrobial resistance. *Clin Microbiol Rev* 31:e00088-17.
- 454 9. Ramos JL, Duque E, Huertas MJ, Haïdour A. 1995. Isolation and expansion of the catabolic  
455 potential of a *Pseudomonas putida* strain able to grow in the presence of high concentrations  
456 of aromatic hydrocarbons. *J Bacteriol* 177:3911–3916.

- 457 10. Shintani M, Sanchez ZK, Kimbara K. 2015. Genomics of microbial plasmids: classification and  
458 identification based on replication and transfer systems and host taxonomy. *Front Microbiol*  
459 6:242.
- 460 11. Hartmans S, van der Werf MJ, de Bont JA. 1990. Bacterial degradation of styrene involving a  
461 novel flavin adenine dinucleotide-dependent styrene monooxygenase. *Appl Environ Microbiol*  
462 56:1347–1351.
- 463 12. Kieboom J, Dennis JJ, de Bont JAM, Zylstra GJ. 1998. Identification and Molecular  
464 Characterization of an Efflux Pump Involved in *Pseudomonas putida* S12 Solvent Tolerance. *J*  
465 *Biol Chem* 273:85–91.
- 466 13. Kusumawardhani H, Hosseini R, de Winde JH. 2018. Solvent Tolerance in Bacteria: Fulfilling the  
467 Promise of the Biotech Era? *Trends Biotechnol* 36:1025–1039.
- 468 14. Mukhopadhyay A. 2015. Tolerance engineering in bacteria for the production of advanced  
469 biofuels and chemicals. *Trends Microbiol* 23:498–508.
- 470 15. Janardhan Garikipati SVB, Peeples TL. 2015. Solvent resistance pumps of *Pseudomonas putida*  
471 S12: Applications in 1-naphthol production and biocatalyst engineering. *J Biotechnol* 210:91–  
472 99.
- 473 16. Koopman F, Wierckx N, de Winde JH, Ruijsenaars HJ. 2010. Efficient whole-cell  
474 biotransformation of 5-(hydroxymethyl)furfural into FDCA, 2,5-furandicarboxylic acid.  
475 *Bioresour Technol* 101:6291–6296.
- 476 17. Verhoef S, Wierckx N, Westerhof RGM, de Winde JH, Ruijsenaars HJ. 2009. Bioproduction of  
477 p-hydroxystyrene from glucose by the solvent-tolerant bacterium *Pseudomonas putida* S12 in  
478 a two-phase water-decanol fermentation. *Appl Environ Microbiol* 75:931–936.
- 479 18. Verhoef S, Ruijsenaars HJ, de Bont JAM, Wery J. 2007. Bioproduction of p-hydroxybenzoate  
480 from renewable feedstock by solvent-tolerant *Pseudomonas putida* S12. *J Biotechnol* 132:49–  
481 56.
- 482 19. Wierckx NJP, Ballerstedt H, de Bont JAM, Wery J. 2005. Engineering of solvent-tolerant  
483 *Pseudomonas putida* S12 for bioproduction of phenol from glucose. *Appl Environ Microbiol*

- 484 71:8221–8227.
- 485 20. Kieboom J, Dennis JJ, Zylstra GJ, de Bont JA. 1998. Active efflux of organic solvents by  
486 *Pseudomonas putida* S12 is induced by solvents. J Bacteriol 180:6769–6772.
- 487 21. Volkers RJM, Snoek LB, Ruijsenaars HJ, de Winde JH. 2015. Dynamic Response of  
488 *Pseudomonas putida* S12 to Sudden Addition of Toluene and the Potential Role of the Solvent  
489 Tolerance Gene *trgl*. PLoS One 10:e0132416.
- 490 22. Rühl J, Hein E-M, Hayen H, Schmid A, Blank LM. 2012. The glycerophospholipid inventory of  
491 *Pseudomonas putida* is conserved between strains and enables growth condition-related  
492 alterations. Microb Biotechnol 5:45–58.
- 493 23. Wijte D, van Baar BLM, Heck AJR, Altelaar AFM. 2011. Probing the proteome response to  
494 toluene exposure in the solvent tolerant *Pseudomonas putida* S12. J Proteome Res 10:394–  
495 403.
- 496 24. Volkers RJM, de Jong AL, Hulst AG, van Baar BLM, de Bont JAM, Wery J. 2006. Chemostat-based  
497 proteomic analysis of toluene-affected *Pseudomonas putida* S12. Environ Microbiol 8:1674–  
498 1679.
- 499 25. Kuepper J, Ruijsenaars HJ, Blank LM, de Winde JH, Wierckx N. 2015. Complete genome  
500 sequence of solvent-tolerant *Pseudomonas putida* S12 including megaplasmid pTTS12. J  
501 Biotechnol 200:17–18.
- 502 26. Volkers RJM, Ballerstedt H, de Winde JH, Ruijsenaars HJ. 2010. Isolation and genetic  
503 characterization of an improved benzene-tolerant mutant of *Pseudomonas putida* S12. Environ  
504 Microbiol Rep 2:456–460.
- 505 27. Wery J, Hidayat B, Kieboom J, de Bont JA. 2001. An insertion sequence prepares *Pseudomonas*  
506 *putida* S12 for severe solvent stress. J Biol Chem 276:5700–5706.
- 507 28. Sun X, Dennis JJ. 2009. A Novel Insertion Sequence Derepresses Efflux Pump Expression and  
508 Preadapts *Pseudomonas putida* S12 for Extreme Solvent Stress. J Bacteriol 191:6773–6777.
- 509 29. Rodríguez-Herva JJ, García V, Hurtado A, Segura A, Ramos JL. 2007. The *ttgGHI* solvent efflux  
510 pump operon of *Pseudomonas putida* DOT-T1E is located on a large self-transmissible plasmid.

- 511 Environ Microbiol 9:1550–1561.
- 512 30. Köhler KAK, Rückert C, Schatschneider S, Vorhölter FJ, Szczepanowski R, Blank LM, Niehaus K,  
513 Goesmann A, Pühler A, Kalinowski J, Schmid A. 2013. Complete genome sequence of  
514 *Pseudomonas sp.* strain VLB120 a solvent tolerant, styrene degrading bacterium, isolated from  
515 forest soil. J Biotechnol 168:729–730.
- 516 31. Stothard P, Wishart DS. 2005. Circular genome visualization and exploration using CGView.  
517 Bioinformatics 21:537–539.
- 518 32. Christie PJ, Whitaker N, González-Rivera C. 2014. Mechanism and structure of the bacterial  
519 type IV secretion systems. Biochim Biophys Acta - Mol Cell Res 1843:1578–1591.
- 520 33. Monchy S, Benotmane MA, Janssen P, Vallaeyts T, Taghavi S, Van Der Lelie D, Mergeay M. 2007.  
521 Plasmids pMOL28 and pMOL30 of *Cupriavidus metallidurans* are specialized in the maximal  
522 viable response to heavy metals. J Bacteriol 189:7417–7425.
- 523 34. Zobel S, Benedetti I, Eisenbach L, de Lorenzo V, Wierckx N, Blank LM. 2015. Tn7-Based Device  
524 for Calibrated Heterologous Gene Expression in *Pseudomonas putida*. ACS Synth Biol 4:1341–  
525 1351.
- 526 35. Taylor DE. 1999. Bacterial tellurite resistance. Trends Microbiol 7:111–115.
- 527 36. Kieboom J, de Bont JAM. 2001. Identification and molecular characterization of an efflux  
528 system involved in *Pseudomonas putida* S12 multidrug resistance. Microbiology 147:43–51.
- 529 37. Hall JPJ, Harrison E, Lilley AK, Paterson S, Spiers AJ, Brockhurst MA. 2015. Environmentally co-  
530 occurring mercury resistance plasmids are genetically and phenotypically diverse and confer  
531 variable context-dependent fitness effects. Environ Microbiol 17:5008–5022.
- 532 38. Jacoby GA, Sutton L, Knobel L, Mammen P. 1983. Properties of IncP-2 plasmids of *Pseudomonas*  
533 *spp.* Antimicrob Agents Chemother 24:168–175.
- 534 39. Harrison E, Brockhurst MA. 2012. Plasmid-mediated horizontal gene transfer is a  
535 coevolutionary process. Trends Microbiol 20:262–267.
- 536 40. Panke S, Witholt B, Schmid A, Wubbolts MG. 1998. Towards a biocatalyst for (S)-styrene oxide  
537 production: characterization of the styrene degradation pathway of *Pseudomonas sp.* strain

- 538 VLB120. *Appl Environ Microbiol* 64:2032–2043.
- 539 41. Li PL, Hwang I, Miyagi H, True H, Farrand SK. 1999. Essential components of the Ti plasmid trb  
540 system, a type IV macromolecular transporter. *J Bacteriol* 181:5033–5041.
- 541 42. Nagai H, Kubori T. 2011. Type IVB secretion systems of *Legionella* and other gram-negative  
542 bacteria. *Front Microbiol* 2:136.
- 543 43. Kusumawardhani H, van Dijk D, Hosseini R, de Winde JH. 2020. A novel toxin-antitoxin module  
544 SlvT–SlvA regulates megaplasmid stability and incites solvent tolerance in *Pseudomonas putida*  
545 S12. *Appl Environ Microbiol* 86:e00686-20.
- 546 44. Turner PE, Cooper VS, Lenski RE. 1998. Tradeoff Between Horizontal and Vertical Modes of  
547 Transmission in Bacterial Plasmids. *Evolution (N Y)* 52:315–329.
- 548 45. R. Craig MacLean, Milan AS. 2015. Microbial Evolution: Towards Resolving the Plasmid Paradox.  
549 *Curr Biol* 25:R764–R767.
- 550 46. Martínez-García E, Benedetti I, Hueso A, de Lorenzo V. 2015. Mining Environmental Plasmids  
551 for Synthetic Biology Parts and Devices. *Microbiol Spectr* 3:PLAS-0033-2014.
- 552 47. Sprouffske K, Wagner A. 2016. Growthcurver: An R package for obtaining interpretable metrics  
553 from microbial growth curves. *BMC Bioinformatics* 17:172.
- 554 48. Martínez-García E, de Lorenzo V. 2011. Engineering multiple genomic deletions in Gram-  
555 negative bacteria: analysis of the multi-resistant antibiotic profile of *Pseudomonas putida*  
556 KT2440. *Environ Microbiol* 13:2702–2716.
- 557 49. Medema MH, Takano E, Breitling R. 2013. Detecting sequence homology at the gene cluster  
558 level with multigeneblast. *Mol Biol Evol* 30:1218–1223.
- 559 50. Katoh K, Standley DM. 2013. MAFFT multiple sequence alignment software version 7:  
560 Improvements in performance and usability. *Mol Biol Evol* 30:772–780.
- 561 51. Edgar RC. 2004. MUSCLE: A multiple sequence alignment method with reduced time and space  
562 complexity. *BMC Bioinformatics* 5:113.
- 563 52. Bethesda Research Laboratories. 1986. *E. coli* DH5 alpha competent cells. *Focus - Bethesda Res*  
564 *Lab* 8:9.

- 565 53. Herrero M, De Lorenzo V, Timmis KN. 1990. Transposon vectors containing non-antibiotic  
566 resistance selection markers for cloning and stable chromosomal insertion of foreign genes in  
567 gram-negative bacteria. *J Bacteriol* 172:6557–6567.
- 568 54. Boyer HW, Roulland-dussoix D. 1969. A complementation analysis of the restriction and  
569 modification of DNA in *Escherichia coli*. *J Mol Biol* 41:459–472.
- 570 55. Bagdasarian M, Lurz R, Rückert B, Franklin FCH, Bagdasarian MM, Frey J, Timmis KN. 1981.  
571 Specific-purpose plasmid cloning vectors II. Broad host range, high copy number, RSF 1010-  
572 derived vectors, and a host-vector system for gene cloning in *Pseudomonas*. *Gene* 16:237–247.
- 573 56. Figurski DH, Helinski DR. 1979. Replication of an origin-containing derivative of plasmid RK2  
574 dependent on a plasmid function provided in trans. *Proc Natl Acad Sci* 76:1648–1652.
- 575 57. Choi K-H, Gaynor JB, White KG, Lopez C, Bosio CM, Karkhoff-Schweizer RR, Schweizer HP. 2005.  
576 A Tn7-based broad-range bacterial cloning and expression system. *Nat Methods* 2:443–448.  
577  
578  
579



## 580 Tables & Figures

581 **Table 1. List of 50 plasmids with the highest similarity scores to pTTS12. pTTS12 coding sequences**

582 **(CDS) were aligned to other megaplasmids available at NCBI databases. The relative similarity score**

583 **was calculated by dividing total scores for each plasmid by total score obtained for pTTS12 itself.**

Rank	Strain	Plasmid	Taxid	Length (bp)	Relative similarity
	<i>Pseudomonas putida</i> S12	pTTS12	1215087	583900	100.00%
1	<i>Pseudomonas aeruginosa</i> PA96	pOZ176	1457392	500839	72.54%
2	<i>Pseudomonas aeruginosa</i> strain FFUP_PS_37	pJB37	287	464804	69.30%
3	<i>Pseudomonas aeruginosa</i> strain AR_0356	unnamed2	287	438531	67.97%
4	<i>Pseudomonas aeruginosa</i> strain AR441	unnamed3	287	438529	66.23%
5	<i>Pseudomonas putida</i> strain SY153	pSY153-MDR	303	468170	64.70%
6	<i>Pseudomonas aeruginosa</i> strain T2436	pBT2436	287	422811	64.69%
7	<i>Pseudomonas koreensis</i> strain P19E3	p1	198620	467568	64.44%
8	<i>Pseudomonas putida</i> strain 12969	p12969-DIM	303	409102	64.43%
9	<i>Pseudomonas aeruginosa</i> strain T2101	pBT2101	287	439744	64.43%
10	<i>Pseudomonas aeruginosa</i> strain PA298	pBM908	287	395774	63.99%
11	<i>Pseudomonas aeruginosa</i> isolate RW109	RW109	287	555265	63.75%
12	<i>Pseudomonas aeruginosa</i> strain PA121617	pBM413	287	423017	63.20%
13	<i>Pseudomonas aeruginosa</i> strain PABL048	pPABL048	287	414954	62.82%
14	<i>Pseudomonas aeruginosa</i>	p727-IMP	287	430173	62.75%
15	<i>Pseudomonas aeruginosa</i> strain AR439	unnamed2	287	437392	62.00%
16	<i>Pseudomonas citronellolis</i> strain SJTE-3	pRBL16	53408	370338	61.12%
17	<i>Pseudomonas aeruginosa</i>	p12939-PER	287	496436	60.86%
18	<i>Pseudomonas aeruginosa</i>	pA681-IMP	287	397519	59.50%
19	<i>Pseudomonas aeruginosa</i>	pR31014-IMP	287	374000	55.58%
20	<i>Pseudomonas taiwanensis</i> VLB120	pSTY	69328	321653	21.65%
21	<i>Pseudomonas fluorescens</i> SBW25	pQBR103	216595	425094	20.48%
22	<i>Pseudomonas syringae</i> pv. <i>maculicola</i> str. ES4326	pPma4326F	629265	387260	20.16%
23	<i>Pseudomonas putida</i> strain KF715	pKF715A	303	483376	16.63%
24	<i>Pseudomonas stutzeri</i> strain YC-YH1	pYCY1	316	225945	16.06%
25	<i>Pseudomonas fluorescens</i> SBW25	pQBR57	216595	307330	14.45%
26	<i>Pseudomonas aeruginosa</i> strain PA83	unnamed1	287	398087	14.42%
27	<i>Pseudomonas aeruginosa</i> strain DN1	unnamed1	287	317349	14.24%
28	<i>Pseudomonas monteilii</i> strain FDAARGOS_171	unnamed	76759	60588	13.85%
29	<i>Salmonella enterica</i> strain 8025	p8025	28901	311280	11.99%
30	<i>Pseudomonas luteola</i> strain FDAARGOS_637	unnamed1	47886	585976	10.92%
31	<i>Enterobacter hormaechei</i> subsp. <i>steigerwaltii</i> strain 34998	p34998	299766	239973	10.39%
32	<i>Enterobacter hormaechei</i> strain A1	pInchI2-1502264	158836	309444	10.37%

33	<i>Leclercia adecarboxylata</i> strain Lec-476	pLec-476	83655	311758	10.06%
34	<i>Enterobacter hormaechei</i> subsp. <i>hoffmannii</i> strain AR_0365	unnamed1	1812934	328871	9.98%
35	<i>Azospira</i> sp. I09	pAZI09	1765049	397391	9.98%
36	<i>Citrobacter freundii</i> strain SL151	unnamed1	546	229406	9.89%
37	<i>Cupriavidus metallidurans</i> strain FDAARGOS_675	unnamed3	119219	2586495	9.54%
38	<i>Cupriavidus metallidurans</i> CH34	megaplasmid	266264	2580084	9.53%
39	<i>Enterobacter hormaechei</i> subsp. <i>hormaechei</i> strain 34983	p34983	301105	328905	9.41%
40	<i>Escherichia coli</i> strain CFSAN064035	pGMI17-003_1	562	310064	9.19%
41	<i>Pseudomonas</i> sp. XWY-1	pXWY	2069256	394537	9.15%
42	<i>Klebsiella oxytoca</i> strain CAV1374	pKPC_CAV1374	571	332956	9.12%
43	<i>Pseudomonas veronii</i> 1YdBTEX2	pPVE	1295141	373858	9.06%
44	<i>Pantoea</i> sp. PSNIH2	pPSP-75c	1484157	378808	9.04%
45	<i>Klebsiella michiganensis</i> strain AR375	unnamed2	1134687	340462	8.96%
46	<i>Citrobacter freundii</i> complex sp. CFNIH9	pCFR-eb27	2077149	355789	8.82%
47	<i>Ralstonia solanacearum</i> strain HA4-1	HA4-1MP	305	1947245	8.82%
48	<i>Enterobacteriaceae</i> bacterium ENNIH1	pENT-1f0b	2066051	302640	8.78%
49	<i>Leclercia</i> sp. LSNIH1	pLEC-1cb1	1920114	341250	8.74%
50	<i>Leclercia</i> sp. LSNIH3	pLEC-7c0d	1920116	330021	8.74%

584

585

586

587

588 **Table 2. Bacterial strains and plasmids used in this study**

Strain/plasmid	Relevant characteristics	References
<i>E. coli</i> DH5 $\alpha$	<i>sup</i> E44, $\Delta$ <i>lacU169</i> ( $\Phi$ <i>lacZ</i> $\Delta$ M15), <i>recA1</i> , <i>endA1</i> , <i>hsdR17</i> , <i>thi-1</i> , <i>gyrA96</i> , <i>relA1</i>	(52)
<i>E. coli</i> DH5 $\alpha$ $\lambda$ pir	<i>sup</i> E44, $\Delta$ <i>lacU169</i> ( $\Phi$ <i>lacZ</i> $\Delta$ M15), <i>recA1</i> , <i>endA1</i> , <i>hsdR17</i> , <i>thi-1</i> , <i>gyrA96</i> , <i>relA1</i> , $\lambda$ pir phage lysogen	(53)
<i>E. coli</i> HB101	<i>recA pro leu hsdR</i> Sm <sup>R</sup>	(54)
<i>E. coli</i> XL-1 Blue	<i>endA1 gyrA96(nalR) thi-1 recA1 relA1 lac glnV44 F'</i> [ <i>::Tn10 proAB+ lacIq <math>\Delta</math>(lacZ)M15</i> ] <i>hsdR17(rk- mK+)</i> Tc <sup>R</sup>	Stratagene
<i>E. coli</i> MV1190	<i>delta(lac-proAB) thi supE44 delta(sr1-recA)306::Tn10 [F':traD36 proAB lacIq delta(lacZ)M15]</i> Tc <sup>R</sup>	ATCC
<i>P. putida</i> KT2440	Derived from wild-type <i>P. putida</i> mt-2, $\Delta$ pWW0	(55)
<i>P. putida</i> S12	Wild-type <i>P. putida</i> S12 (ATCC 700801), harboring megaplasmid pTTS12	(11)
<i>P. putida</i> S12.1	<i>P. putida</i> S12; Km <sup>R</sup> on pTTS12	This paper
<i>P. putida</i> KT-BG35	<i>P. putida</i> KT2440; Gm <sup>R</sup> , <i>msfgfp::Tn7</i>	This paper
<i>P. putida</i> KTpS12	<i>P. putida</i> KT2440, Gm <sup>R</sup> , <i>msfgfp::Tn7</i> , pTTS12, Km <sup>R</sup>	This paper
pRK2013	RK2-Tra <sup>+</sup> , RK2-Mob <sup>+</sup> , Km <sup>R</sup> , <i>ori</i> ColE1	(56)
pTTS12	A 583 kbp megaplasmid of <i>P. putida</i> S12	(25)
pTnS-1	Ap <sup>R</sup> , <i>ori</i> R6K, TnSABCD operon	(57)
pBG35	Km <sup>R</sup> , Gm <sup>R</sup> , <i>ori</i> R6K, pBG-derived	(34)
pEMG	Km <sup>R</sup> , Ap <sup>R</sup> , <i>ori</i> R6K, <i>lacZ</i> $\alpha$ MCS flanked by two I-SceI sites	(48)

589

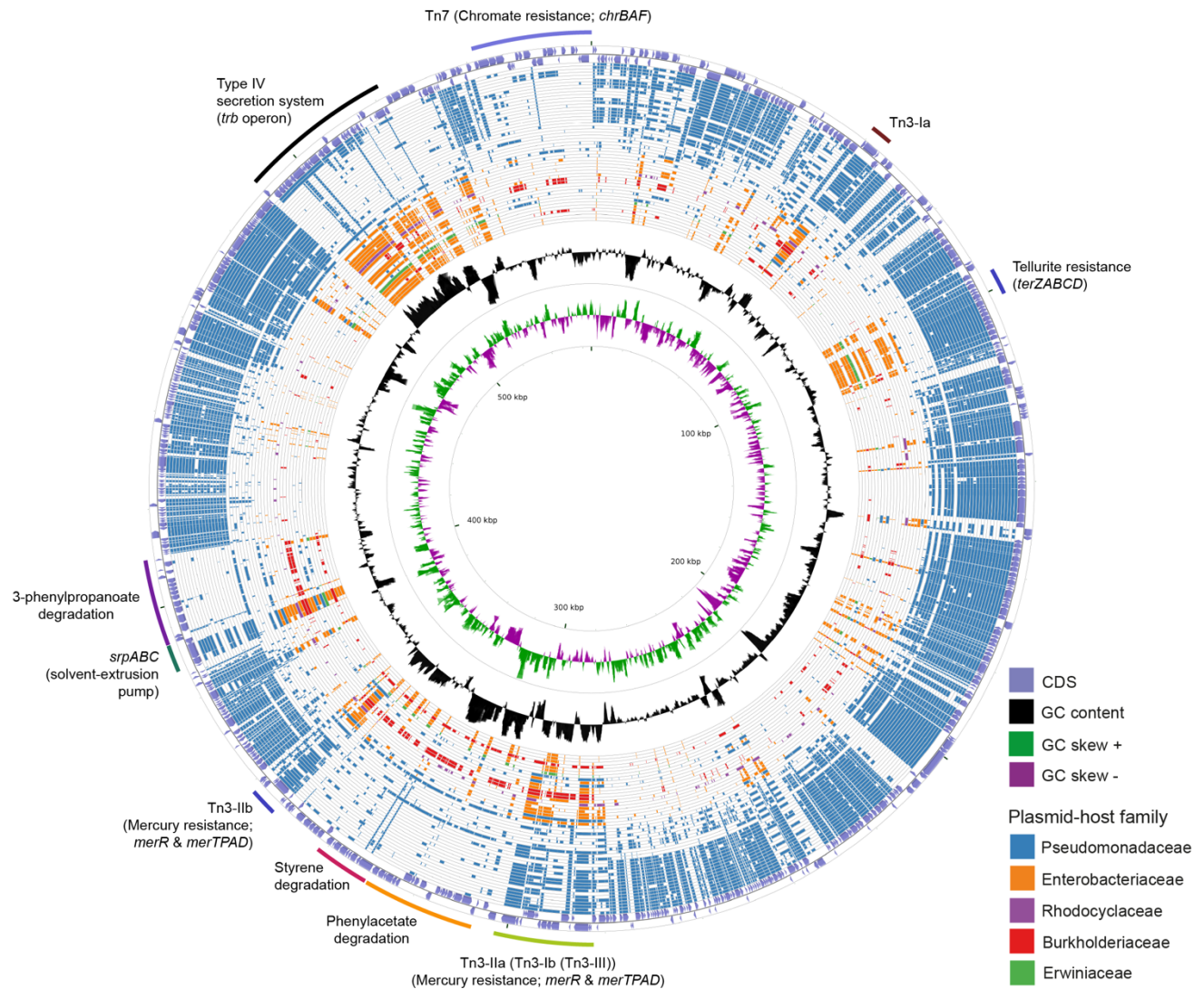
590

591 **Table 3. Primers used in this study**

Primer	Sequence	Target
glmS_Fw	AGTCAGAGTTACGGAATTGTAGG	<i>P. putida</i> KT2440 (Tn7 site)
glmS_Rv	GTCGAGAAAATTGCCGAGCT	<i>P. putida</i> KT2440 (Tn7 site)
53,496_Fw	ACTTCGACCAATGCCCCATT	<i>P. putida</i> S12 pTTS12
56,596_Rv	GGACACCCTCATCCTTAGCG	<i>P. putida</i> S12 pTTS12
200,497_Fw	GTGTATCGAAGGGCCTCCAC	<i>P. putida</i> S12 pTTS12
203,602_Rv	TCGACGATGCAGACAGATCG	<i>P. putida</i> S12 pTTS12
286,448_Fw	AACACCGAAGATGGGGCTTT	<i>P. putida</i> S12 pTTS12
289,462_Rv	GCAGGTCGACAAGCAAGTTG	<i>P. putida</i> S12 pTTS12
4,963,661_Fw	ATCACCCAGCTGAGCCATTC	<i>P. putida</i> S12 chromosome
4,966,726_Rv	CTGCCGATAACAAAGCAGC	<i>P. putida</i> S12 chromosome
90285_Fw	TTT <b>TCTAGAT</b> GCTGAGCAGTTCCTCAGG	Construction of pEMG-TS for Km <sup>R</sup> marker in pTTS12, with XbaI restriction site
90825_Rv	TTT <b>CCCGGG</b> AGGAAGGGAAGCAAACCTCCG	Construction of pEMG-TS for Km <sup>R</sup> marker in pTTS12, with XmaI restriction site
TS1_28750_Fw	AATCT <b>GAATTC</b> GGACGTATTGGGCTTCAATG	Construction of pEMG-Δ28750 for deleting the putative relaxase, with EcoRI restriction site
TS1_28750_Rv	GAAAGCCTGTCTGCACATGGCTATCGACTCATCATTACCG	Construction of pEMG-Δ28750 for deleting the putative relaxase
TS2_28750_Fw	CGGTGAATGATGAGTCGATCATGTGCAGACAGGCTTTC	Construction of pEMG-Δ28750 for deleting the putative relaxase
TS2_28750_Rv	AACCC <b>GGATCC</b> GTTTCGACAGCCGCTATTTTC	Construction of pEMG-Δ28750 for deleting the putative relaxase, with BamHI restriction site
test_28750_Fw	CCTGATGCACGATTTACCG	Confirming the deletion of the putative relaxase (ΔRPPX_28750)
test_28750_Rv	CTACCTGCCGGTACACATT	Confirming the deletion of the putative relaxase (ΔRPPX_28750)

592

593



594

595 **Figure 1. Circular plot of the top 50 plasmids with the highest identity scores to pTTS12**

596 pTTS12 coding sequences (CDS) were aligned to 28915 other plasmids available at NCBI Refseq and

597 Nucleotide databases. The outer light purple ring represents the CDS of plus and minus strand of pTTS12.

598 In the inner ring, the GC content is represented in black and the positive and negative GC skew are

599 represented in green and purple respectively. The plasmids are ordered based on their similarity and

600 coverage to pTTS12 CDS from outermost to innermost of the plot with each ring representing a single

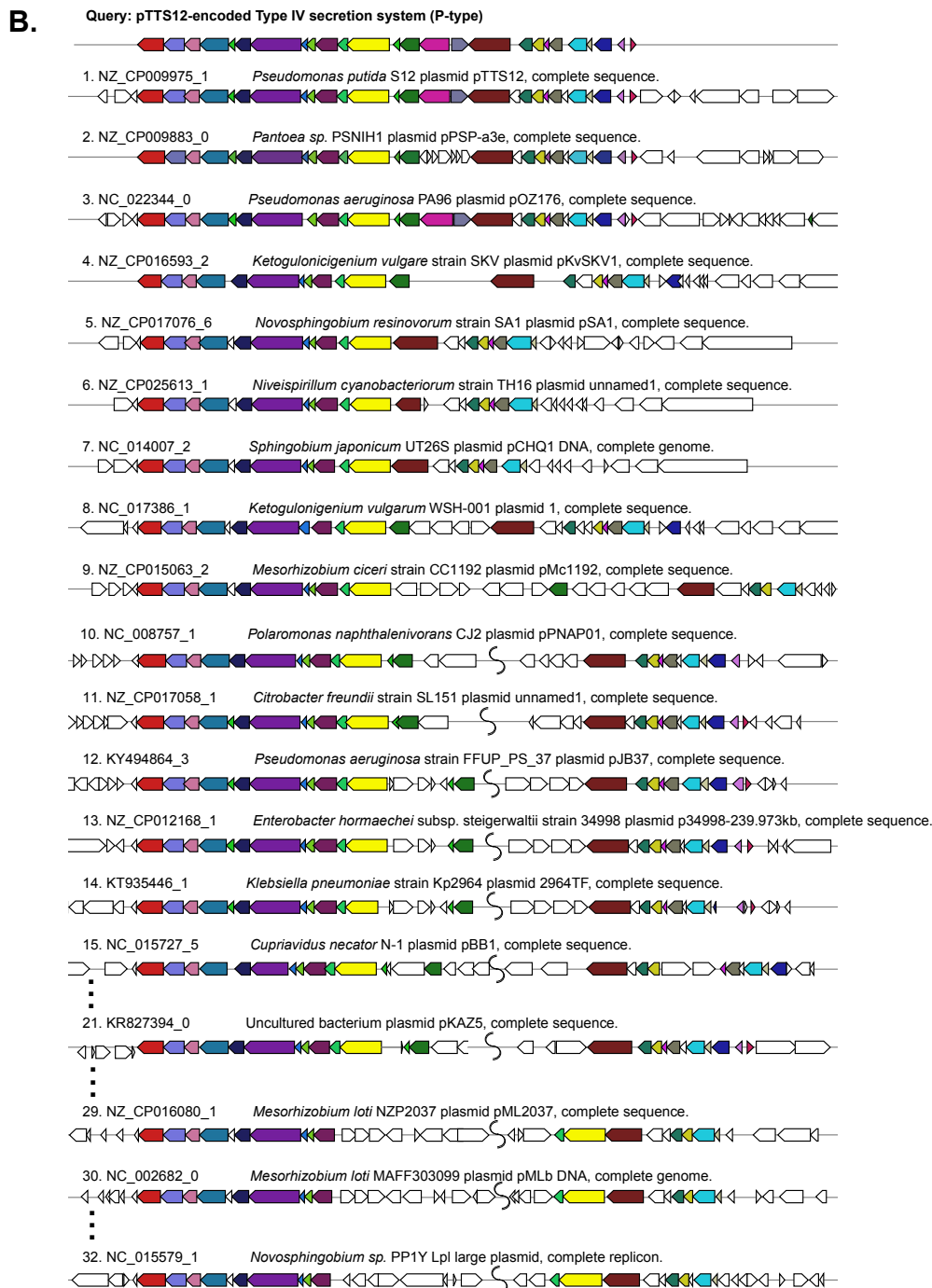
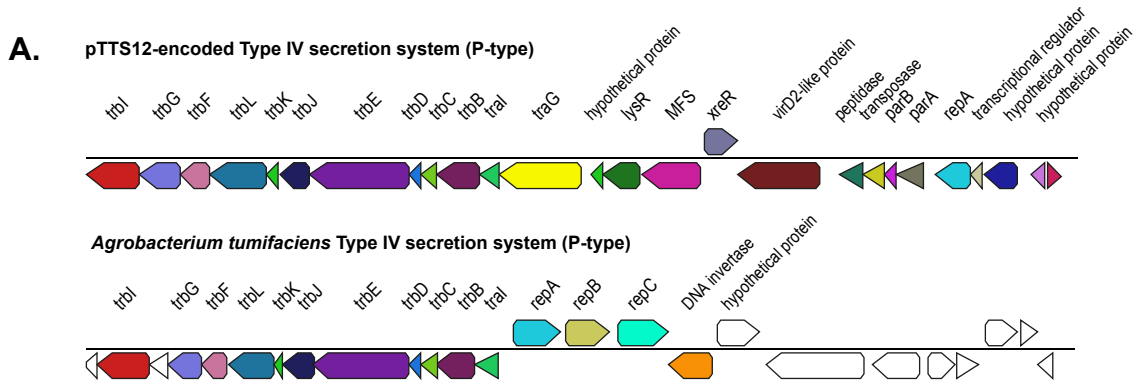
601 plasmid as listed in Table 1. Ring colors represent different plasmid-host families; Pseudomonadaceae

602 (blue), Enterobacteriaceae (orange), Rhodocyclaceae (purple), Burkholderiaceae (red), and

603 Erwiniaceae (green). The position of the gene clusters of interest are annotated in the figure. An

604 extended circular plot of the top 500 plasmids with highest identity scores to pTTS12 are shown in

605 Figure S1.



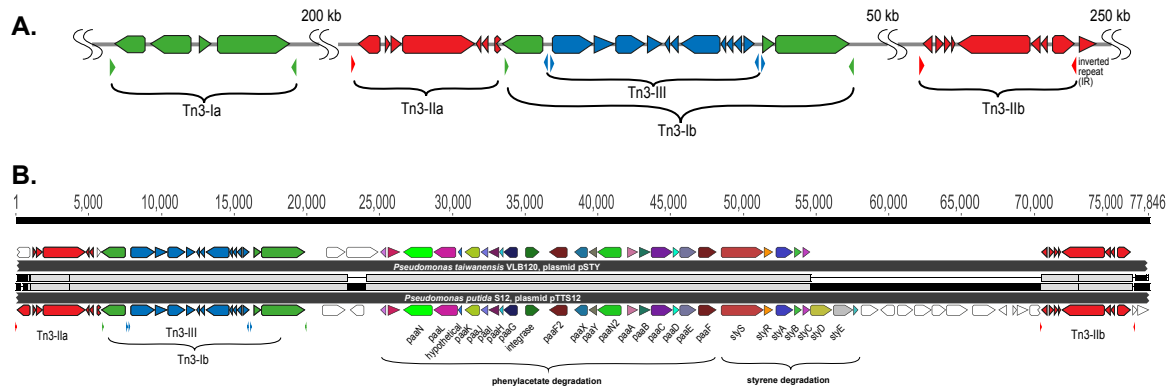
607 **Figure 2. Structure and synteny of pTTS12 conjugation system**

608 A. The arrangement of the T4SS gene cluster found in pTTS12 and the prototype *trb* operon from  
609 *Agrobacterium tumefaciens* (pTiC58). The colors represent different genes in the cluster and same  
610 colors are assigned for the homologous genes. The gene names are indicated above the respective  
611 clusters. pTTS12/T4SS and the *trb* operon of pTiC58 share synteny for 11 genes (*trbI* to *traiI*), while  
612 other parts are clearly different.

613 B. Synteny plot of the T4SS gene cluster of pTTS12 for plasmid conjugation, replication and partitioning  
614 compared with other plasmids. This visualization was generated using multigeneblast software (49).  
615 The numbers refer to the order of decreasing synteny. For the sake of clarity, several plots were  
616 removed from this figure, indicated by the dots. The colors represent different genes in the cluster  
617 corresponding to color-coding in panel A. Putative coupling-protein (T4CP) *traG* is indicated in yellow  
618 and the putative relaxase *virD2*-like protein is indicated in brown.

619

620



621

622 **Figure 3. Tn3 transposon family elements responsible for horizontal gene transfer of styrene and**  
 623 **phenylacetate degradation pathway.**

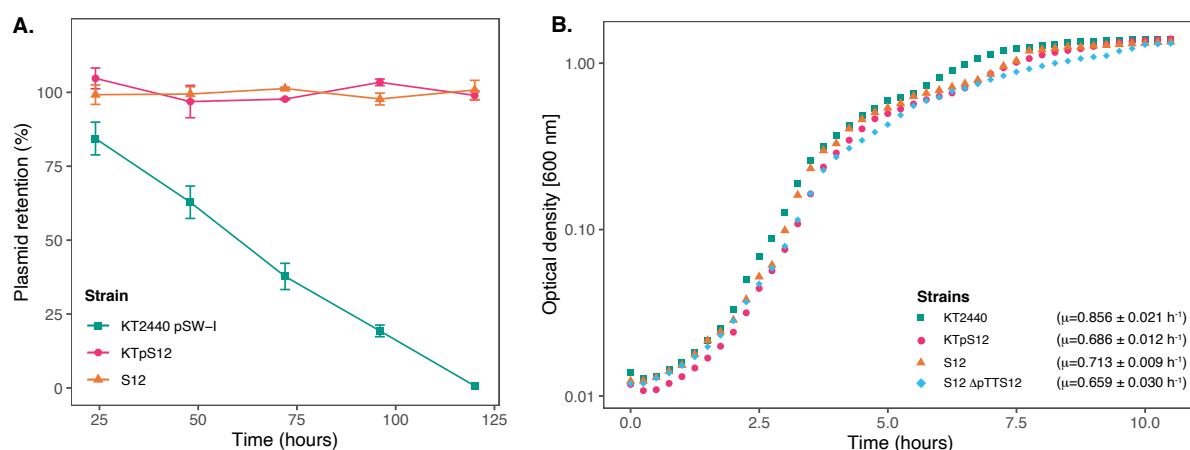
624 A. Genetic organization of the three different Tn3-family transposable elements in pTTS12. Colors  
 625 represent the three different Tn3 transposon families; Tn3-I with highest identity to Tn4656 (green),  
 626 Tn3-IIa and b with highest identity to Tn5053 (red) and Tn3-III with highest identity to Tn5563 (blue) .  
 627 The inverted repeats (IRs) flanking each element are marked by small lowered triangles in the same  
 628 colours, accordingly.

629 B. Alignment of the Tn3-mediated horizontal gene transfer of the styrene and phenylacetate  
 630 degradation cluster in pTTS12 (bottom) and pSTY from *Pseudomonas taiwanensis* VLB120 (top). Colors  
 631 represent the different genes constituting styrene-phenylacetate degradation cluster and the three  
 632 Tn3 transposable elements, corresponding to the color-coding in panel A. Gene names are indicated.

633

634





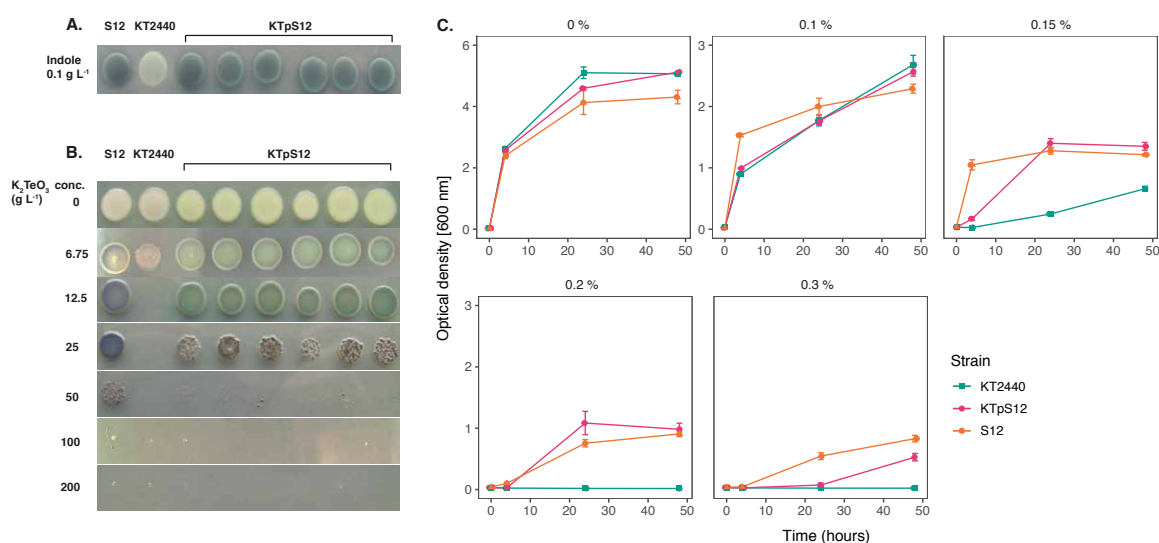
635

636 **Figure 4. Megaplasmid pTTS12 is highly stable in *P. putida* strains and reduces maximal growth rate**  
 637 **in *P. putida* KT2440.**

638 A. Plasmid retention of pTTS12 in *P. putida* KT2440 and *P. putida* S12 on liquid LB without selection  
 639 pressure for approximately 50 generations. Colors and shapes indicate the different strains with green  
 640 squares indicating *P. putida* KT2440 pSW-II, magenta circles indicating *P. putida* KTpS12, and orange  
 641 triangles indicating *P. putida* S12 (containing pTTS12). Plasmid pSW-II in *P. putida* KT2440 was used as  
 642 a control for loss of unstable plasmid. pTTS12 is stably maintained in both *P. putida* S12 and *P. putida*  
 643 KTpS12.

644 B. Growth curve of *P. putida* KT2440, *P. putida* KTpTTS12, *P. putida* S12, and *P. putida* S12 ΔpTTS12.  
 645 Growth was followed on liquid LB at 30 °C, 200 rpm shaking. Growth curves represent data obtained  
 646 from three biological replicates for each strain, starting from OD<sub>600nm</sub> = 0.05. Green squares indicate  
 647 *P. putida* KT2440 pSW-II, magenta circles indicate *P. putida* KTpS12, orange triangles indicate *P. putida*  
 648 S12 (containing pTTS12), and blue diamonds indicate *P. putida* S12 ΔpTTS12. Maximum growth rates  
 649 calculated for each strain are indicated within the figure.

650



651

652 **Figure 5. Transfer of pTTS12 phenotypic characteristics.**

653 A. Production of indigo from indole indicating activity of styrene monooxygenase (StyA) and styrene  
 654 oxide isomerase (StyB). Minimal medium (M9) was supplemented with indole which, in the presence  
 655 of StyAB enzymes encoded on pTTS12, is converted into indigo. Positive control *P. putida* S12 showed  
 656 indigo coloration, whereas negative control *P. putida* KT2440 remained white. *P. putida* KTpS12  
 657 showed indigo coloration indicating activity of pTTS12-encoded *styAB*.

658 B. Growth of *P. putida* strains in the presence of potassium tellurite (K<sub>2</sub>TeO<sub>3</sub>). Minimum inhibitory  
 659 concentration (MIC) of positive control *P. putida* S12 was 200 g L<sup>-1</sup> whereas the MIC of the wild-type  
 660 *P. putida* KT2440 was 12.5 g L<sup>-1</sup>. The MIC of *P. putida* KTpS12 was 100 g L<sup>-1</sup> indicating the presence and  
 661 activity of the *ter* operon on pTTS12.

662 C. Growth of *P. putida* strains on increasing concentrations of toluene. Optical density (OD<sub>600nm</sub>) of the  
 663 cultures was measured at 4, 24, and 48-hour time points with starting point of OD<sub>600nm</sub> = 0.1. The y-  
 664 axis range is different between the first panel (0-6) and the other panels (0-3). Green squares indicate  
 665 *P. putida* KT2440 pSW-II, magenta circles indicate *P. putida* KTpS12, and orange triangles indicate *P.*  
 666 *putida* S12 (containing pTTS12). *P. putida* KTpS12 showed an increase in solvent tolerance indicating  
 667 the presence and activity of the *srp* operon from pTTS12.

668